NeuroImage: Clinical 35 (2022) 103085

Contents lists available at ScienceDirect

NeuroImage: Clinical

journal homepage: www.elsevier.com/locate/ynicl

Neurite density of white matter significantly correlates with tuberous sclerosis complex disease severity

Debbie Anaby [a,b,*], Shai Shrot [a,b], Eugenia Belenky [a,b], Bruria Ben-Zeev [b,c], Michal Tzadok [b,c]

[a] Department of Diagnostic Imaging, Sheba Medical Center, Tel HaShomer, Israel
[b] Sackler School of Medicine, Tel Aviv University, Tel Aviv, Israel
[c] Pediatric Neurology Institute, Sheba Medical Center, Tel HaShomer, Israel

ARTICLE INFO

Keywords:
Tuberous sclerosis complex
Diffusion tensor imaging
Neurite orientation and dispersion imaging
White matter

ABSTRACT

Objective: To assess whether white matter (WM) diffusion tensor imaging (DTI) and neurite orientation dispersion and density imaging (NODDI) derived measures correlate with tuberous sclerosis complex (TSC) disease severity.
Cohort and methods: A multi-shell diffusion protocol was added to the clinical MRI brain scans of thirteen patients including 6 males and 7 females with a mean ± std age of 17.2 ± 5.8 years. Fractional anisotropy (FA) and mean diffusivity (MD) were generated from DTI and neurite density index (NDI), orientation dispersion index (ODI) and free water index (fiso) were generated from NODDI. A clinical score was determined for each patient according to the existence of epilepsy, developmental delay, autism or psychiatric disorders. Whole-brain segmented WM was averaged for each parametric map and 3 group k-means clustering was performed on the NDI and FA maps. MRI quantitative parameters were correlated with the clinical scores.
Results: Segmented whole brain WM averages of MD and NDI values showed significant negative ($p = 0.0058$) and positive ($p = 0.0092$) correlations with the clinical scores, respectively. Additionally, the contribution of the low and high NDI-based clusters to the whole brain WM significantly correlated with the clinical scores ($p = 0.03$ and $p = 0.00047$, respectively). No correlation was found when the clusters were based on the FA maps.
Conclusion: Advanced diffusion MRI of TSC patients revealed widespread WM alterations. Neurite density showed significant correlations with disease severity and is therefore suggested to reflect an underlying biological process in TSC WM. The quantification of WM alterations by advanced diffusion MRI may be an additional biomarker for TSC and may be advantageous as a complementary MR protocol for the evaluation of TSC patients.

1. Introduction

Tuberous sclerosis is a rare autosomal dominant disorder with an incidence of one in 6,000–10,000. Mutations in TSC1 or TSC2 lead to the development of numerous benign or malignant neoplasms, in multiple organ systems. Neurological manifestations are present in >95% of TSC patients and are usually the cause for morbidity and mortality (Orlova and Crino, 2010). Therefore, neuroimaging for early diagnosis, regular surveillance and follow-up is crucial. Brain microstructural alterations include cortical tubers, white matter (WM) lesions, subependymal nodules (SENs) and subependymal giant cell astrocytoma (SEGAs) (Orlova and Crino, 2010). These are preferably diagnosed and followed-up by MRI, which is considered the common imaging method for an accurate characterization of the CNS involvement in TSC.

The clinical manifestations are unpredictable and highly diverse with varying severity. These may include epilepsy, neurocognitive dysfunction, psychiatric disorders and developmental disorders such as autism and intellectual disability (Mühlebner et al., 2020; Orlova and Crino, 2010).

The correlation between neuroimaging findings and neurological manifestations in TSC is not fully understood. Cortical tubers are considered indicative of TSC and have been investigated for a correlation with neurological deficits, however, results were found to be variable and indefinite (Chifari, 2020; Kaczorowska et al., 2011; O'Callaghan et al., 2004; Simao et al., 2010). More recently, studies were shifted towards the investigation of WM abnormalities in TSC and their contribution to neurological symptoms, based on the hypothesis that WM alterations and abnormal circuitry can affect intellectual impairment and autism. The WM may be affected by a combination of several microstructural alterations including demyelination, axon loss,

* Corresponding author at: Department of Diagnostic Imaging, Sheba Medical Center, Tel HaShomer, Israel.
E-mail address: debbie.anaby@sheba.health.gov.il (D. Anaby).

https://doi.org/10.1016/j.nicl.2022.103085
Received 20 February 2022; Received in revised form 11 May 2022; Accepted 13 June 2022
Available online 22 June 2022

gliosis and inflammation (Soo et al., 2015). Studies in TSC1 or TSC2 mutated mice have shown that the axon specification, guidance and myelination are abnormal (Choi et al., 2008; Meikle et al., 2007; Nie et al., 2010). In human patients with TSC, normal-appearing WM has been studied mainly with diffusion tensor MRI (DT-MRI), in which WM abnormalities were detected (Dogan et al., 2016; Im et al., 2016; Kurtcan et al., 2018; Peters et al., 2013; Prohl et al., 2019). However, a change in the DTI-derived measures such as fractional anisotropy (FA) can be indicated by several underlying pathologies such as changes in axonal diameter, fiber density, myelination etc. Therefore, DTI is considered a non-specific measure of microstructural characterization, providing parameters that cannot be attributed to specific biophysical factors. Advanced diffusion techniques are constantly being developed with the aim of improving the specificity and providing more accurate characterization of brain tissue.

Neurite orientation dispersion and density imaging (NODDI) is a clinically feasible advanced diffusion MRI technique developed by Zhang et al. (2012). The model is based on biophysical properties of the tissue, consisting of three individual compartments; intra-cellular, extra-cellular and cerebrospinal fluid (CSF). The MR signal from each of the compartments is separate and the full MR signal in each voxel is a combination of all three compartments. The intra-cellular compartment refers to the neurites and is modeled as a set of 'sticks' that are considered to be highly restricted and may be coherent, fanned or sprawled, such that the orientation dispersion of the neurites may range from being highly parallel to highly dispersed. The model for this compartment is based on restricted anisotropic non-Gaussian diffusion. The extra-cellular compartment refers mainly to the glial cells and its water diffusion is considered to be hindered. It is modeled with Gaussian anisotropic diffusion. The CSF compartment is modeled as isotropic Gaussian diffusion (Zhang et al., 2012). The main measures provided by NODDI are neurite density index (NDI), neurite orientation dispersion index (ODI) and free water compartment (fiso). Whole brain parametric maps of these measures were shown to be consistent with the known brain anatomy. NDI values are higher in WM than in gray matter (GM), especially in dense and packed WM tracts. ODI is higher in GM than in WM, where neurites are less coherent or relatively fanned. The corpus callosum, for example, exhibits high NDI and low ODI values. Fiso values are highest in CSF regions like the ventricles (Zhang et al., 2012). The separation of the three compartments in the NODDI model allows to disentangle factors that contribute to DTI-derived FA. For example, a reduction in neurite density and an increase in orientation dispersion both result in a reduction of FA. Therefore, NODDI-derived measures are considered to be more specific and accurate than the DT-MRI derived measures for the evaluation of microstructural changes. WM abnormalities are known to occur in TSC, however, no obvious biological interpretation can be given based on conventional MRI or DTI. The use of NODDI may provide a more specific characterization of the tissue microstructural changes in TSC with biophysical meaningful parameters. A recent study of NODDI in TSC patients indicated that NDI is decreased in widespread regions in the brain but no correlation of any of the NODDI or DTI derived metrics with clinical symptoms was found (Taoka et al., 2020). The current study aimed to further explore WM microstructural alterations in TSC and attempted to attribute those changes to a specific biological process. Further, the correlation of advanced diffusion MRI derived-measureswith disease severity was observed.

2. Methods

2.1. Study population

The study group included 13 TSC diagnosed patients which are regularly followed up in the TSC clinic in the Sheba Medical Center. TSC diagnosis was based on genetic analysis in 12/13 patients. In one patient, TSC diagnosis was based on clinical and radiological findings. An advanced diffusion MRI scan was added to the clinical MR scan. Patients who were too young or incapable were sedated. The hospital ethical review board approved the study and informed consent forms were signed by the patients/guardians prior to the MRI scans.

2.2. MRI acquisition

MRI data were collected using a 3T Siemens PRISMA (Siemens Healthcare, Erlangen, Germany) with a 20 channel head coil at the Department of Diagnostic Imaging in Sheba. The scan includeda full clinical protocol and a multi-shell diffusion sequence. The conventional scans included T1-weighted magnetization-prepared rapid gradient-echo (MPRAGE) with TR/TE = 2100/2.45 ms, FOV = 25.6x25.6 cm, voxel size = 1x1x1 mm; T2-weighted turbo spin-echo with TR/TE = 3750/100 ms, FOV = 24x24 cm, voxel size = 0.5x0.5x4 mm; 3D fluid-attenuated inversion recovery (FLAIR) with TR/TE = 5000/315 ms, FOV = 25.6x25.6 mm, voxel size = 0.5x0.5x1 mm. The multi-shell diffusion protocol was performed with TR/TE = 4000/66 ms, 4 b0 images, 64 directions with each of the b-values; 1000 s/mm^2 and 2000 s/mm^2, FOV = 172 × 224 mm, voxel size = 2 × 2 × 2 mm and multi-band, provided by the Center for Magnetic Resonance Research (CMRR, Minneapolis, Minnesota, USA) allowing for a clinically feasible scan time of 9.5 min.

2.3. Image analysis

The diffusion multi-shell data was used for NODDI analysis (https://www.nitrc.org/projects/noddi_toolbox) and the b = 1000 shell data was extracted and used for DTI analysis (ExploreDTI, (Leemans et al., 2009)). NDI, ODI and fiso maps were created from NODDI and FA and MD maps were created from DTI. All maps were co-registered with T1 MPRAGE images segmented to WM, gray matter (GM) and CSF (SPM12, (Friston et al., 1995)). The WM segmented images were binarized (above a threshold of 0.5) and applied to all diffusion derived maps. Additionally, a 3-group k-means cluster analysis (Mathworks R2021b) was performed separately on the WM NDI maps and on the WM FA maps. The number of voxels that constitute each cluster were divided by the total number of WM voxels in order to derive the contribution of each cluster to the total brain WM. These were correlated with the clinical score.

2.4. Clinical score

A clinical score was calculated per patient based on neuropsychologist validated assessments and neurologic and psychiatric evaluations. The main factors that were considered for the evaluation were child-related (age, gender, school placement, psychiatric diagnosis) and epilepsy-related (illness duration, number of antiseizure medications (ASMs), epilepsy type). Cognitive function was evaluated according to indices of visuomotor, executive functions, attention and memory, which were determined by validated neuropsychological tests. Teacher's and parent's report were also considered (Silberg et al., 2020).

Four characteristic phenotypes in TSC were collected from every patient, each donating 1 point to the score if exists or none if does not exist; epilepsy seizures, developmental delay or mental retardation, autism and psychiatric disorders. Patients with no clinical manifestations were given a score of 0 while the highest score was 4.

2.5. Statistical analysis

Average whole-brain WM values from each of the parametric maps (FA, MD, NDI, ODI and fiso) were correlated with the clinical score. The contributions of each of the NDI- or FA-derived clusters were correlated with the clinical score as well. In all cases Spearman correlations were used, with a correction for age (Mathworks R2021b). $p < 0.05$ was considered statistically significant.

3. Results

3.1. Demographics

Table 1 shows the characteristics of the study cohort. Mean age was 17.23 years (SD = 5.85) and 53.8% were female. 83.3% had TSC2 mutation and 16.6% had TSC1 mutation. One subject had none of the clinical symptoms considered for this study, therefore was given a score of 0 (subject #8, Table 1). The rest of the patients suffered from epilepsy (92.3%), all with duration of >5 years. Of them 83.3% had both focal and generalized epilepsy, took more than3 antiseizure medications (ASMs) and attended special education, while 16.6% had only focal epilepsy, took two ASMs and attended mainstream schools. Most patients also suffered from developmental delay or mental retardation (84.6%). Autism and psychiatric disorders were detected in approximately half of the patients (53.8% and 61.5%, respectively).

3.2. Conventional MRI findings

The number of tubers in each hemisphere and in the cerebellum, the existence of SENs and SEGAs and the presence of atrophy were analyzed from the 3D FLAIR images. >5 tubers were found in each hemisphere of most patients and the cerebellum was free of tubers in 10 out of 13 patients. SENs were present in all patients except for one and SEGAs were found in more than half of the patients. Atrophy was detected only in 2 patients. See Table 1 in Supplementary Material.

3.3. Whole-brain white matter correlations with disease score

Representative NODDI- and DTI-derived maps of patients #7 (clinical score 3) and #8 (clinical score 0) are depicted in Fig. 1. Whole-brain WM average values of each parametric measure were correlated with the clinical scores, adjusted for age (Fig. 2). NDI showed a significant decrease with the clinical score and MD showed a significant increase with the clinical score ($r = -0.71$, $p = 0.0092$ and $r = 0.74$, $p = 0.0058$, respectively). The difference in NDI values between mild and severely affected cases is clearly shown in Fig. 1. FA, ODI and fiso did not show significant correlations with the clinical score ($r = -0.34$, $p = 0.28$; $r = -0.12$, $p = 0.71$; $r = 0.25$, $p = 0.43$, respectively).

3.4. The contribution of neurite density based clusters to whole brain white matter

Representative WM segmented images of NDI and FA maps and their clustered maps are shown in Fig. 3. The clustering according to NDI and FA provides a similar partition of the three groups, however not identical (Fig. 3, A1 vs B1). High values of NDI and FA are found mostly in the periventricular WM areas while low values of NDI and FA are found in the borders between WM and GM and in WM lesions (white arrows).

The contribution of each cluster to the whole-brain WM and its correlation with the clinical score was calculated (Fig. 4A, B). The contribution of low and high value clusters derived from the NDI maps were significantly correlated with the clinical score (Fig. 4A). The percentage of voxels associated with the low values (blue) increased with the clinical score and the percentage of the voxels associated with the high values (gray) decreased. An identical analysis, based on the FA maps, did not reveal any significant correlations with the clinical score (Fig. 4B). The cluster contributions were also averaged per clinical score and presented as stack plots (Fig. 4C, D). Here, when the cluster analysis was based on the NDI maps (Fig. 4C) the low values increase from 11.1% (clinical score '0′) to 17.5% (clinical score '4′) and the high values decrease from 35.1% (clinical score, '0′) to 22.1% (clinical score, '4′). The mid values do not show a changing trend throughout the clinical scores. None of the average clusters show a clear trend when the cluster analysis is based on the FA maps (Fig. 4D).

4. Discussion

There are several findings in this study. First, whole-brain WM alterations are well characterized by diffusion-MRI metrics and correlate with disease severity. This is significantly shown with NODDI-derived 'NDI' and with DTI-derived 'MD'. A more profound observation of the WM by k-means clustering of the NDI maps revealed that the contribution of the low NDI cluster significantly increases with the disease severity while the contribution of the high NDI cluster significantly decreases. Thus, NDI is suggested to be an accurate diffusion-based MRI metric for the detection and characterization of TSC WM alterations. Clustering of the FA maps and their correlation with disease severity did not show significance. However, DTI has been shown to reveal WM alterations in TSC in several studies. Usually, FA was found to be decreased, whereas MD or ADC were increased in the abnormal WM (Garaci et al., 2004; Makki et al., 2007; Simao et al., 2010). Some studies searched for correlations of WM alterations with neurological outcomes such as autism (Peters et al., 2011) and epilepsy (Kurtcan et al., 2018), in which DTI measures were found to change significantly and even underconnectivity across multiple WM tracts was found (Prohl et al., 2019). Recently, advanced analysis was performed on the DTI-derived metrics with the aim of observing the whole-brain connectivity in TSC, which was found to be disrupted (Im et al., 2016; Peters et al., 2013; Tsai et al., 2021). However, DTI measures are regarded as non-specific, therefore difficult to interpret. FA may be modulated by several manifestations including demyelination/dysmyelination (Beaulieu, 2002) and axonal damage (Budde and Annese, 2013) such that two major key factors are entangled; 'neurite density' and 'neurite orientation dispersion'. To this

Table 1
Clinical characteristics of the TSC patients.

Patient	Sex	Age [years]	Genetics	Clinical score	Epilepsy duration [years]	Number of ASMs	Epilepsy type	School education	Developmental delay/mental retardation	Autism	Psychiatric disorders
1	F	11	TSC2	4	>5	>3	Focal and generalized	Special	†	†	†
2	F	11	TSC1	1	>5	2	Focal	Mainstream	–	–	–
3	F	12	TSC2	2	>5	>3	Focal and generalized	Special	†	–	–
4	M	12	TSC2	4	>5	>3	Focal and generalized	Special	†	†	†
5	M	14	TSC2	3	>5	>3	Focal and generalized	Special	†	†	–
6	F	15	TSC1	2	>5	>3	Focal and generalized	Special	†	–	–
7	F	16	TSC2	3	>5	>3	Focal and generalized	Special	†	–	†
8	F	16	TSC2	0	–	–	–	Mainstream	–	–	–
9	M	19	TSC2	4	>5	>3	Focal and generalized	Special	†	†	†
10	M	19	TSC2	4	>5	>3	Focal and generalized	Special	†	†	†
11	F	25	–	4	>5	>3	Focal and generalized	Special	†	†	†
12	M	26	TSC2	2	>5	2	Focal	Mainstream	–	–	†
13	M	28	TSC2	3	>5	>3	Focal and generalized	Special	†	†	†

M – male, F - female.

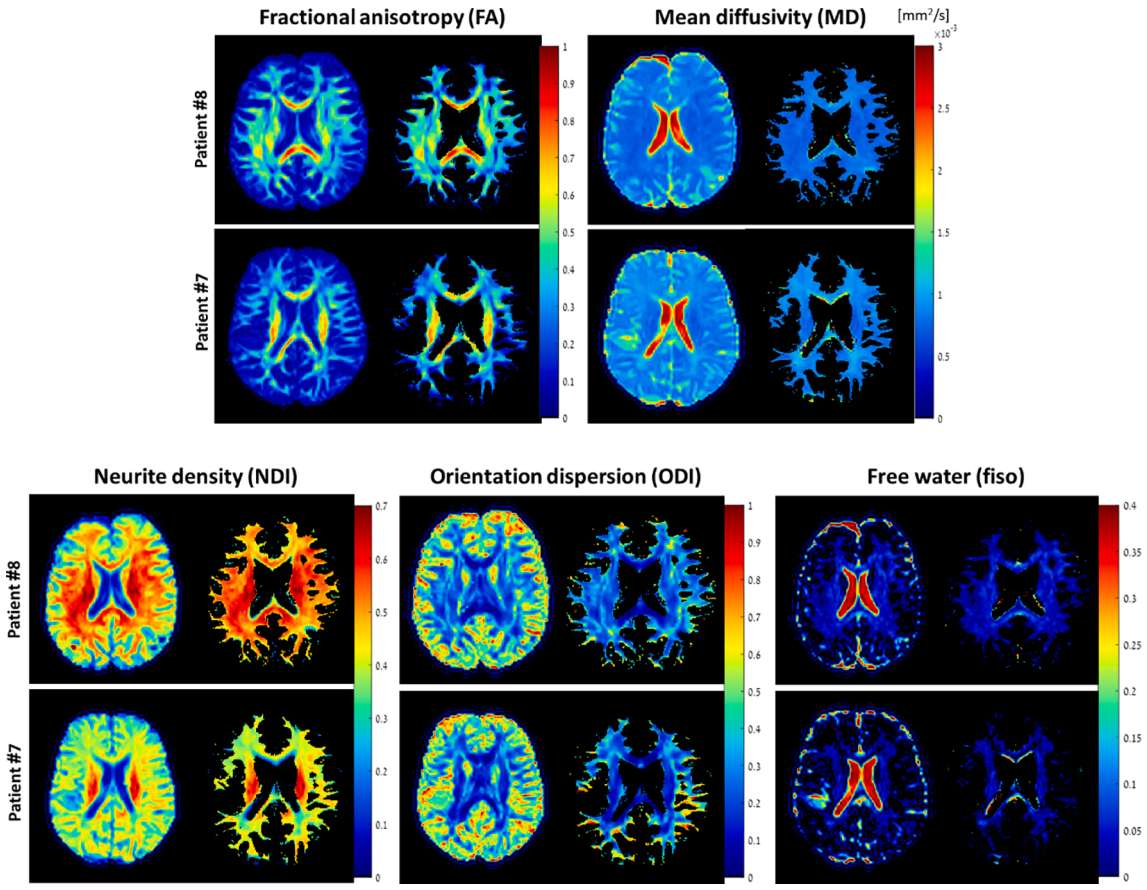

Fig. 1. DTI-derived maps of FA and MD and NODDI-derived maps of NDI, ODI and fiso along with their segmented WM from patients #7 and #8 (Table 1). FA seems thin and sparse, with somewhat lower values in patient #7 than patient #8. MD values are lower in patient #8 than in patient #7. The NODDI-derived maps clearly show a reduction in WM NDI in patient #7, while ODI also seems mildly reduced. Fiso values do not show a clear difference between the two patients, although the number of voxels showing a free water fraction is reduced in patient #7 compared with patient #8.

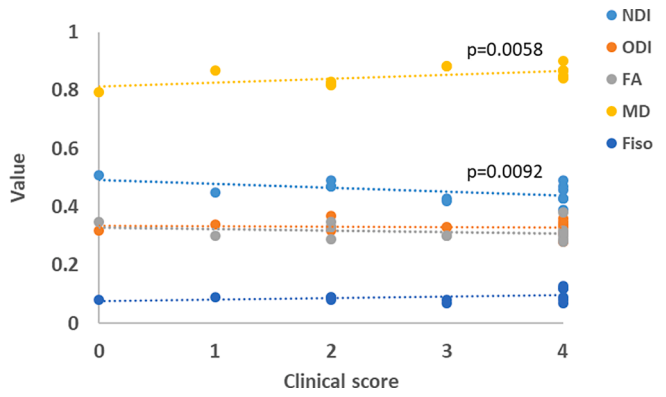

Fig. 2. Partial correlations between whole brain WM NODDI- and DTI-derived metrics and clinical score. NDI and MD showed significant correlations.

end, advanced diffusion MR models, which provide specific measures, may be important for an improved understanding of the microstructural alterations in TSC WM and their underlying biological process. One such study was conducted recently showing that NDI reveals more widespread WM abnormalities as compared to DTI measures but no correlations with clinical symptoms were found (Taoka et al., 2020).

Herein, we aimed to quantitatively characterize the WM microstructural changes in TSC using NODDI and observe whether its measures are significantly correlated with a clinical score. WM was evaluated objectively by automatic whole-brain segmentation and cluster analysis considering the microstructural alterations' widespread nature and location variability. The patients' whole-brain WM was inspected by averaging the WM segmented maps generated from both DTI and NODDI and correlating the values with the disease score. Results showed that even when taking a whole-brain WM average, a significant correlation exists between two diffusion measures and the disease score. This is in line with the diffuse nature of the WM microstructural alterations in TSC, as shown in several studies (Im et al., 2016; Prohl et al., 2019; Wong et al., 2013). Localized microstructural alterations in specific WM could have been averaged out and missed in a whole-brain averaging approach and would not necessarily show significance. MD and NDI were significantly correlated with the clinical score, while the other metrics were not, including FA. Whole-brain WM averaged MD significantly increased with the clinical score, as expected and in line with previous studies that showed larger MD values in TSC compared with control patients (Baumer et al., 2018; Makki et al., 2007), while the averaged NDI significantly decreased with the clinical score. These NDI changes suggest that neurite density may be the dominant underlying biological derangement in the WM of TSC patients rather than neurite orientation dispersion which did not show significance. Interestingly, Zhang et al. (2012) showed that FA is influenced more strongly by neurite orientation dispersion than neurite density. The fact that FA did not change significantly with disease severity could be related to the fact that neurite orientation dispersion did not change significantly either. In order to further observe the WM microstructural changes in more specific regions, yet independent of a pre-determined tract selection, a 3-group k-means cluster analysis was performed based on the NDI and the FA maps. We hypothesized that the

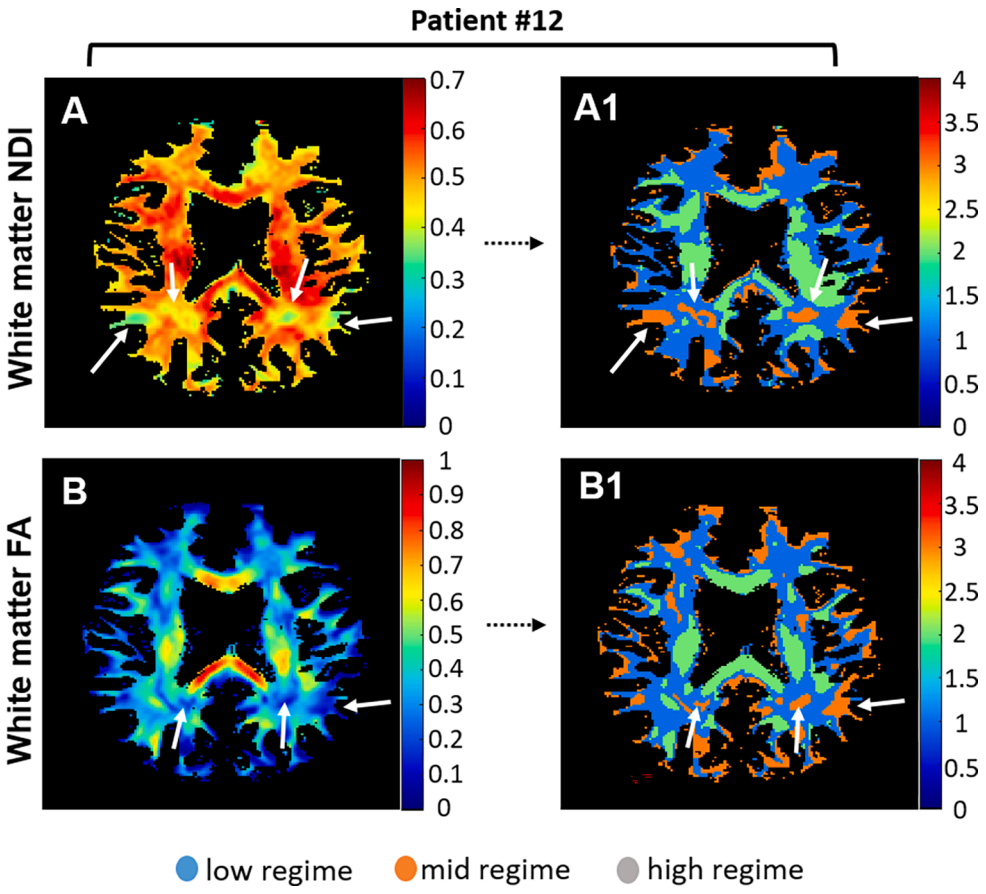

Fig. 3. WM NDI and FA representative maps of patient 12 (A & B, respectively) along with their clustered maps (A1 & B1, respectively).

proportions between the number of voxels contained in each cluster would differ depending on the clinical score, i.e., patients with a more severe disease would show more NDI voxels of low value than patients with a mild disease. Indeed, the WM of patients with a more severe disease (clinical scores 3 or 4) contained more voxels associated with the low NDI values cluster and fewer voxels associated with the high NDI values cluster than the mild patients (Fig. 4). The percentage of voxels in the low and high value NDI-based clusters was significantly correlated with the clinical score. The FA-based clusters did not show the expected trends with no significant correlations with the clinical score.

The present study had several limitations. First, the study group included a relatively small number of patients. As a consequence, the MRI indices were correlated with a general clinical score rather than specific clinical features. Additionally, MRI indices were averaged throughout the whole brain WM or clustered into three areas, while specific locations of WM microstructural changes were not observed. Also, the small group did not allow a comparison between TSC1 and TSC2 patients, in terms of the affected regions or clinical manifestations. Quantitative MR-derived indices like total brain volume and tuber volume were shown to be different between patients with TSC1 and TSC2 mutations in previous studies (Ogórek et al., 2020; Robinson et al., 2022), therefore, it would be interesting to observe these groups with advanced diffusion-derived indices. Another limitation is the wide age range of the study group. This was considered in the statistical analysis, however, a larger group of patients in a narrow age range would be favorable. Note that a group of healthy controls was not scanned in the current study because the aims were to correlate the MRI findings with disease severity. Finally, the user dependent specification of the number of clusters is a limitation of k-means clustering. Three clusters were chosen according to the severely affected patients, in which a very low NDI value cluster was assumed to exist in addition to two higher value clusters.

The results of this study suggest that NODDI-derived indices may have a potential in accurately characterizing brain abnormalities in TSC, significantly correlated with disease severity. Subsequent studies, including larger groups of patients should be performed in order to further explore our findings including correlations with specific clinical characteristics like cognitive development and psychiatric symptoms, observation of abnormality locations, comparison of MRI findings between TSC1 and TSC2 mutated patients and NODDI's potential in MRI follow-up of patients. Importantly, in contrast to other epileptic encephalopathies, in TSC, mammalian target of rapamycin (mTOR) inhibitors can be used to interfere with the biologic mechanism and influence the epilepsy severity and cognitive development, therefore prognostic MRI indices may be advantageous.

In conclusion, our study showed that whole-brain WM alterations are correlated with disease severity, therefore a WM quantitative assessment may be important for the evaluation of TSC patients, in addition to the conventional neuroradiological assessment. Additionally, neurite density was found to accurately characterize white matter alterations in TSC, suggesting that it is a dominant underlying biological process in this disease.

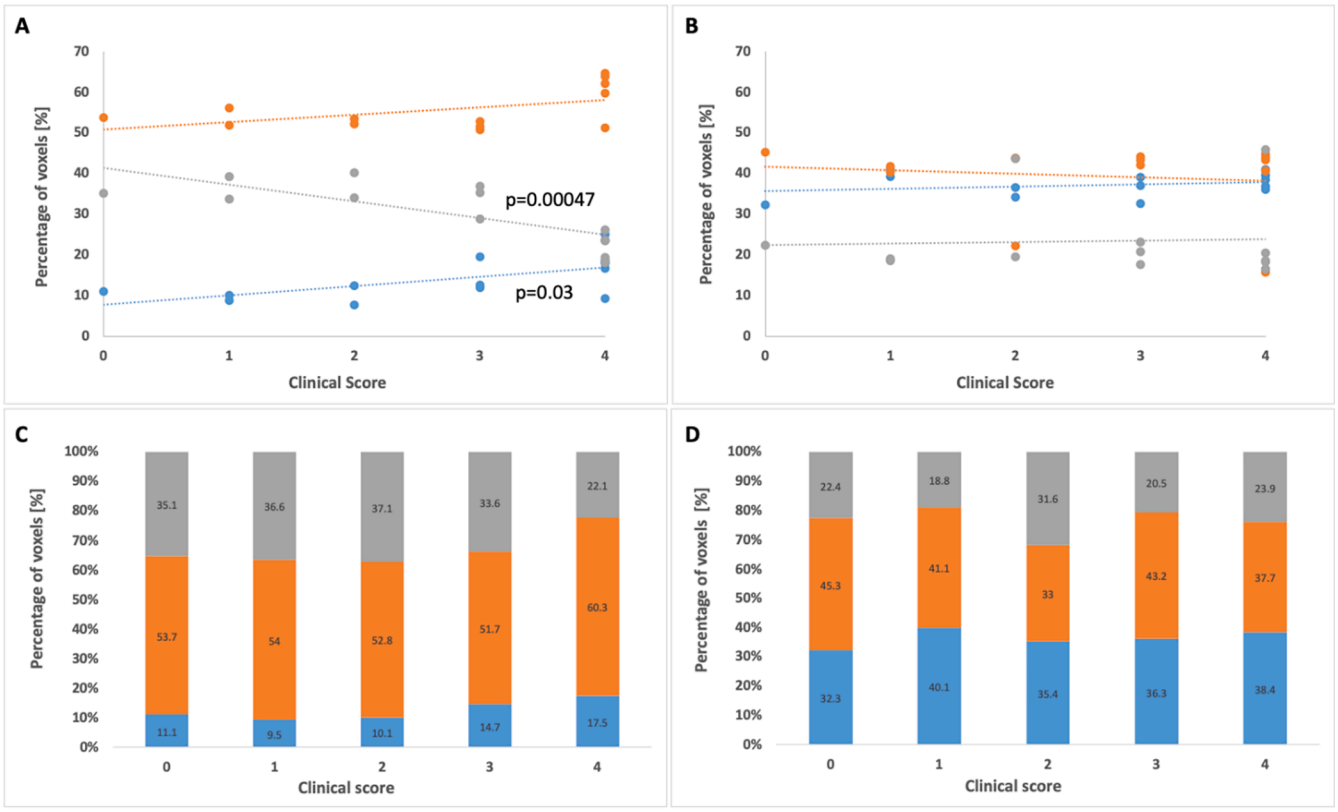

Fig. 4. Spearman correlations of cluster voxel percentages out of whole-brain white matter, adjusted for age, according to NDI (A) and FA (B). The cluster voxel percentages were averaged per clinical score and their contribution to the total is shown as a stack plot; according to NDI (C) and FA (D) maps. Significance was defined as $p < 0.05$.

CRediT authorship contribution statement

Debbie Anaby: Conceptualization, Methodology, Software, Formal analysis, Investigation, Writing – original draft, Visualization. **Shai Shrot:** Conceptualization, Writing – original draft. **Eugenia Belenky:** Investigation. **Bruria Ben-Zeev:** Writing – review & editing. **Michal Tzadok:** Conceptualization, Investigation, Resources, Writing – review & editing.

Declaration of Competing Interest

The authors declare that they have no known competing financial interests or personal relationships that could have appeared to influence the work reported in this paper.

Appendix A. Supplementary data

Supplementary data to this article can be found online at https://doi.org/10.1016/j.nicl.2022.103085.

References

Baumer, F.M., Peters, J.M., Clancy, S., Prohl, A.K., Prabhu, S.P., Scherrer, B., Jansen, F. E., Braun, K.P.J., Sahin, M., Stamm, A., Warfield, S.K., 2018. Corpus callosum white matter diffusivity reflects cumulative neurological comorbidity in tuberous sclerosis complex. Cereb. Cortex 28, 3665–3672. https://doi.org/10.1093/cercor/bhx247.

Beaulieu, C., 2002. The basis of anisotropic water diffusion in the nervous system - A technical review. NMR Biomed. 15 (7-8), 435–455.

Budde, M.D., Annese, J., 2013. Quantification of anisotropy and fiber orientation in human brain histological sections. Front. Integr. Neurosci. https://doi.org/10.3389/fnint.2013.00003.

Chifari, R., 2020. Lack of Correlation between Tuber Number and Cognitive Level in Mild TSC Patients : a Clinical and Genetic Study 1, 20–24.

Choi, Y.J., Di Nardo, A., Kramvis, I., Meikle, L., Kwiatkowski, D.J., Sahin, M., He, X., 2008. Tuberous sclerosis complex proteins control axon formation. Genes Dev. 22, 2485–2495. https://doi.org/10.1101/gad.1685008.

Dogan, M.S., Gumus, K., Koc, G., Doganay, S., Per, H., Gorkem, S.B., Canpolat, M., Bayram, A.K., Coskun, A., 2016. Brain diffusion tensor imaging in children with tuberous sclerosis. Diagn. Interv. Imaging 97, 171–176. https://doi.org/10.1016/j.diii.2015.04.002.

Friston, K.J., Ashburner, J., Frith, C.D., Poline, J.-B., Heather, J.D., Frackowiak, R.S.J., 1995. Spatial registration and normalization of images. Hum. Brain Mapp. 3, 165–189. https://doi.org/10.1002/hbm.460030303.

Garaci, F.G., Floris, R., Bozzao, A., Manenti, G., Simonetti, A., Lupattelli, T., Curatolo, P., Simonetti, G., 2004. Increased brain apparent diffusion coefficient in tuberous sclerosis. Radiology 232, 461–465. https://doi.org/10.1148/radiol.2322030198.

Im, K., Ahtam, B., Haehn, D., Peters, J.M., Warfield, S.K., Sahin, M., Ellen Grant, P., 2016. Altered Structural Brain Networks in Tuberous Sclerosis Complex. Cereb. Cortex 26, 2046–2058. https://doi.org/10.1093/CERCOR/BHV026.

Kaczorowska, M., Jurkiewicz, E., Domanska-Pakiela, D., Syczewska, M., Lojszczyk, B., Chmielewski, D., Kotulska, K., Kuczynski, D., Kmieć, T., Dunin-Wasowicz, D., Kasprzyk-Obara, J., Jozwiak, S., 2011. Cerebral tuber count and its impact on mental outcome of patients with tuberous sclerosis complex. Epilepsia 52 (1), 22–27.

Kurtcan, S., Alkan, A., Guler, S., Yesil, G., Toprak, H., Tüzün, U., Yetis, H., Aralasmak, A., Ozdemir, H., Iscan, A., 2018. The Contribution of DTI in Determining the Relationship of Epilepsy and Brain Lesions in Children with Tuberous Sclerosis. Health Qual. Life Outcomes 9. https://doi.org/10.1186/1477-7525-9-118.

Leemans, A., Jeurissen, B., Sijbers, J., Jones, D., 2009. ExploreDTI: a graphical toolbox for processing, analyzing, and visualizing diffusion MR data. Proc. 17th Sci. Meet. Int. Soc. Magn. Reson. Med. 17, 3537.

Makki, M.I., Chugani, D.C., Janisse, J., Chugani, H.T., 2007. Characteristics of abnormal diffusivity in normal-appearing white matter investigated with diffusion tensor MR imaging in tuberous sclerosis complex. Am. J. Neuroradiol. 28, 1662–1667. https://doi.org/10.3174/ajnr.A0642.

Meikle, L., Talos, D.M., Onda, H., Pollizzi, K., Rotenberg, A., Sahin, M., Jensen, F.E., Kwiatkowski, D.J., 2007. A mouse model of tuberous sclerosis: Neuronal loss of Tsc1 causes dysplastic and ectopic neurons, reduced myelination, seizure activity, and limited survival. J. Neurosci. 27, 5546–5558. https://doi.org/10.1523/JNEUROSCI.5540-06.2007.

Mühlebner, A., Van Scheppingen, J., De Neef, A., Bongaarts, A., Zimmer, T.S., Mills, J.D., Jansen, F.E., Spliet, W.G.M., Krsek, P., Zamecnik, J., Coras, R., Blumcke, I., Feucht, M., Scholl, T., Gruber, V.E., Hainfellner, J.A., Söylemezoğlu, F., Kotulska, K., Lagae, L., Jansen, A.C., Kwiatkowski, D.J., Jozwiak, S., Curatolo, P., Aronica, E., 2020. Myelin pathology beyond white matter in Tuberous Sclerosis Complex (TSC)

cortical tubers. J. Neuropathol. Exp. Neurol. 79, 1054–1064. https://doi.org/10.1093/jnen/nlaa090.

Nie, D., Di Nardo, A., Han, J.M., Baharanyi, H., Kramvis, I., Huynh, T., Dabora, S., Codeluppi, S., Pandolfi, P.P., Pasquale, E.B., Sahin, M., 2010. Tsc2-Rheb signaling regulates EphA-mediated axon guidance. Nat. Neurosci. 13, 163–172. https://doi.org/10.1038/nn.2477.

O'Callaghan, F.J.K., Harris, T., Joinson, C., Bolton, P., Noakes, M., Presdee, D., Renowden, S., Shiell, A., Martyn, C.N., Osborne, J.P., 2004. The relation of infantile spasms, tubers, and intelligence in tuberous sclerosis complex. Arch. Dis. Child. 89, 530–533. https://doi.org/10.1136/adc.2003.026815.

Ogórek, B., Hamieh, L., Hulshof, H.M., Lasseter, K., Klonowska, K., Kuijf, H., Moavero, R., Hertzberg, C., Weschke, B., Riney, K., Feucht, M., Scholl, T., Krsek, P., Nabbout, R., Jansen, A.C., Benova, B., Aronica, E., Lagae, L., Curatolo, P., Borkowska, J., Sadowski, K., Domańska-Pakieła, D., Janson, S., Kozlowski, P., Urbanska, M., Jaworski, J., Jozwiak, S., Jansen, F.E., Kotulska, K., Kwiatkowski, D. J., 2020. TSC2 pathogenic variants are predictive of severe clinical manifestations in TSC infants: results of the EPISTOP study. Genet. Med. 22, 1489–1497. https://doi.org/10.1038/s41436-020-0823-4.

Orlova, K.A., Crino, P.B., 2010. The tuberous sclerosis complex. Ann. N. Y. Acad. Sci. 1184, 87–105. https://doi.org/10.1111/j.1749-6632.2009.05117.x.

Peters, J.M., Sahin, M., Vogel-Farley, V., 2011. Loss of white matter microstructural integrity is associated with adverse neurological outcome in Tuberous Sclerosis Complex Jurriaan 25, 713–724. https://doi.org/10.1016/j.acra.2011.08.016.Loss.

Peters, J.M., Taquet, M., Vega, C., Jeste, S.S., Fernández, I.S., Tan, J., Nelson, C.A., Sahin, M., Warfield, S.K., 2013. Brain functional networks in syndromic and non-syndromic autism: A graph theoretical study of EEG connectivity. BMC Med. 11, 1–16. https://doi.org/10.1186/1741-7015-11-54.

Prohl, A.K., Scherrer, B., Tomas-Fernandez, X., Davis, P.E., Filip-Dhima, R., Prabhu, S.P., Peters, J.M., Bebin, E.M., Krueger, D.A., Northrup, H., Wu, J.Y., Sahin, M., Warfield, S.K., 2019. Early white matter development is abnormal in tuberous sclerosis complex patients who develop autism spectrum disorder. J. Neurodev. Disord. 11, 1–16. https://doi.org/10.1186/s11689-019-9293-x.

Robinson, J., Uzun, O., Loh, N.R., Harris, I.R., Woolley, T.E., Harwood, A.J., Gardner, J. F., Syed, Y.A., 2022. The association of neurodevelopmental abnormalities, congenital heart and renal defects in a tuberous sclerosis complex patient cohort. BMC Med. 20, 1–19. https://doi.org/10.1186/s12916-022-02325-0.

Silberg, T., Ahoniska-Assa, J., Bord, A., Levav, M., Polack, O., Tzadok, M., Heimer, G., Bar-Yosef, O., Geva, R., Ben-Zeev, B., 2020. In the eye of the beholder: Using a multiple-informant approach to examine the mediating effect of cognitive functioning on emotional and behavioral problems in children with an active epilepsy. Seizure 82, 31–38. https://doi.org/10.1016/j.seizure.2020.09.002.

Simao, G., Raybaud, C., Chuang, S., Go, C., Snead, O.C., Widjaja, E., 2010. Diffusion tensor imaging of commissural and projection white matter in tuberous sclerosis complex and correlation with tuber load. Am. J. Neuroradiol. 31, 1273–1277. https://doi.org/10.3174/ajnr.A2033.

Soo, Y., Yang, D., Roe, C.M., Coats, A., 2015. Pathological Correlates of White Matter Hyperintensities on Magnetic Resonance Imaging. Dement. Geriatr. Cogn. Disord. 717, 92–104.

Taoka, T., Aida, N., Fujii, Y., Ichikawa, K., Kawai, H., Nakane, T., Ito, R., Naganawa, S., 2020. White matter microstructural changes in tuberous sclerosis: Evaluation by neurite orientation dispersion and density imaging (NODDI) and diffusion tensor images. Sci. Rep. 10, 1–9. https://doi.org/10.1038/s41598-019-57306-w.

Tsai, J.D., Ho, M.C., Lee, H.Y., Shen, C.Y., Li, J.Y., Weng, J.C., 2021. Disrupted white matter connectivity and organization of brain structural connectomes in tuberous sclerosis complex patients with neuropsychiatric disorders using diffusion tensor imaging. Magn. Reson. Mater. Physics. Biol. Med. 34, 189–200. https://doi.org/10.1007/s10334-020-00870-4.

Wong, A.M., Wang, H.S., Schwartz, E.S., Toh, C.H., Zimmerman, R.A., Liu, P.L., Wu, Y. M., Ng, S.H., Wang, J.J., 2013. Cerebral diffusion tensor MR tractography in tuberous sclerosis complex: Correlation with neurologic severity and tract-based spatial statistical analysis. Am. J. Neuroradiol. 34, 1829–1835. https://doi.org/10.3174/ajnr.A3507.

Zhang, H., Schneider, T., Wheeler-Kingshott, C.A., Alexander, D.C., 2012. NODDI: Practical in vivo neurite orientation dispersion and density imaging of the human brain. Neuroimage 61, 1000–1016. https://doi.org/10.1016/j.neuroimage.2012.03.072.